Title: Mechanical loading influences the viscoelastic performance of the resin-carious dentin complex.

Short title: Viscoelasticity of the resin-dentin interface after load cycling.

Authors: Manuel Toledano[1][*], Raquel Osorio[1], Modesto T. López-López[2], Fátima S. Aguilera[1], Franklin García-Godoy[3], Manuel Toledano-Osorio[1], Estrella Osorio[1].

Institution: [1]University of Granada, Faculty of Dentistry, Dental Materials Section.

[2]University of Granada, Faculty of Science, Applied Physics Department.

[3]Bioscience Research Center, College of Dentistry, University of Tennessee, Memphis.

Address: [1]University of Granada, Faculty of Dentistry, Dental Materials Section. Colegio Máximo de Cartuja s/n 18071 Granada - Spain.

[2]University of Granada, Faculty of Science, Applied Physics Department. Av. Fuente Nueva s/ n 18071 Granada - Spain.

[3]Bioscience Research Center, College of Dentistry, University of Tennessee, Health Science Center, 875 Union Avenue, Memphis. 38163-Tennessee-USA.

*Corresponding author: Prof. Manuel Toledano

University of Granada, Faculty of Dentistry

Dental Materials Section

Colegio Máximo de Cartuja s/n

18071 – Granada - Spain.

Tel.: +34-958243788

Fax: +34-958240809

Email: toledano@ugr.es

Abstract

The aim of this study was to evaluate the changes in the mechanical behavior and bonding capability of Zn-doped resin-infiltrated caries-affected dentin interfaces. Dentin surfaces were treated with 37% phosphoric acid (PA) followed by application of a dentin adhesive, Single Bond (SB) (PA+SB) or by 0.5 M ethylenediaminetetraacetic acid (EDTA) followed by SB (EDTA+SB). 10 wt% ZnO microparticles or 2 wt% $ZnCl_2$ were added into SB, resulting in the following groups: PA+SB, PA+SB-ZnO, PA+SB-$ZnCl_2$, EDTA+SB, EDTA+SB-ZnO, EDTA+SB-$ZnCl_2$. Bonded interfaces were stored for 24 h, and tested or submitted to mechanical loading. Microtensile bond strength was assessed. Debonded surfaces were evaluated by scanning electron microscopy and elemental analysis. The hybrid layer, bottom of the hybrid layer, peritubular and intertubular dentin were evaluated using a nanoindenter. The load/displacement responses were used for the nano-dynamic mechanical analysis (nano-DMA III) to estimate complex modulus, tan delta, loss modulus and storage modulus. The modulus mapping was obtained by imposing a quasistatic force setpoint to which a sinusoidal force was superimposed. AFM imaging was performed. Load cycling decreased the tan delta at the PA+SB-$ZnCl_2$ and EDTA+SB-ZnO interfaces. Tan delta was also diminished at peritubular dentin when PA+SB-ZnO was used, hindering the dissipation of energy throughout these structures. Tan delta increased at the interface after using EDTA+SB-$ZnCl_2$, lowering the energy for recoil or failure. After load cycling, loss moduli at the interface decreased when using $ZnCl_2$ as doping agent, increasing the risk of fracture; but when using ZnO loss moduli was dissimilarly affected if dentin was EDTA-treated. The border between intertubular and peritubular dentin attained the highest discrepancy in values of viscoelastic properties, meaning a risk for cracking and breakdown of the resin-dentin interface. PA used on dentin provoked differences in

complex and storage modulus values at the intertubular and peritubular structures, and these differences were higher than when EDTA was employed. In these cases, the long-term performance of the restorative interface will be impared.

I. INTRODUCTION

Dentin structure is composed of about 50 vol% mineral in the form of a sub-micrometer to nanometer-sized, carbonate rich, calcium deficient apatite crystallites. It is dispersed between parallel, micrometer-sized, hypermineralized, collagen-poor hollow cylinders, and dentinal tubules, containing peritubular dentin. Intertubular dentin occupies the region between the tubules. It consists of an organic matrix (collagen fibrils) reinforced by nanoscopic apatite crystals similar to that of peritubular dentin[1,2]. Dentin represents the most common dental substrate to be used in multiple adhesive techniques for restoration[3]. Dentists usually must bond adhesives to irregular dentin substrates such as carious dentin[4]. Caries-affected dentin should be preserved during clinical treatment because it is remineralizable and serves as a suitable substrate for dentin adhesion. Etch-and-rinse bonding systems act by removing both the smear layer and mineral ions[5] from dentin with phosphoric acid (PA), followed by the application of a primer and an adhesive. This creates the hybrid layer (HL) over a zone of non infiltrated but demineralized collagen substratum (the bottom of the hybrid layer) (BHL). This unprotected collagen may become the site for collagen hydrolysis by host-derived matrix metalloproteinase (MMP) enzymes[6], and should be remineralized. Milder conditioners (*i.e.* ethylenediaminetetraacetic acid -EDTA-) eliminate the smear layer, but remove less calcium from the dentin surface. EDTA promotes a shallow demineralization inducing, as a chelating agent, favorable chemical modifications[7]. EDTA does not alter dentin proteins and their collagen fibrils are thought to retain most of the intrafibrillar mineral content. Nevertheless, even with EDTA agents, it seems that a volume of demineralized and non-resin infiltrated collagen remains at the base (bottom) of the hybrid layer[8]. If effective inhibitors of MMPs are included in resin-

dentin bonding interfaces, they may protect the seed crystallite-sparse collagen fibrils of the scaffold from degradation, and they could be remineralized[9].

Zinc has been demonstrated to reduce MMPs-mediated collagen degradation[6], to inhibit dentin demineralization[10] and to induce dentin remineralization at the bonded interface[11]. It is assumed that the mechanism of action of ZnO particles is based on partial particles dissolution and zinc ions liberation. ZnO is an amphoteric oxide, although normally shows basic properties. It is nearly insoluble in water but its solubility is expected to increase in a biological medium (i.e. at the dentin interface) in which a body fluid solution exists. It has been previously shown that the presence of proteins drastically enhance the dissolution of ZnO particles by binding their peptides to zinc[12,13]. By scanning electron microscope and energy dispersive X-ray analysis of ZnO-doped adhesive bonded dentin surfaces, it was found that ZnO particles penetrate dentinal tubules, but preferentially remained at the bottom of the hybrid layer. They do not penetrate intertubular dentin but remain in direct contact with the demineralized dentin collagen[14]. The deposition of zinc particles at this site will facilitate the effective release of zinc ions and binding to collagen, at the resin-dentin interface.

Numerical modelling of restored teeth to understand load transfer within the tooth and its restorative interface is essential. Viscoelastic materials, such as dentin[15] exhibit time-dependent strain[16,17]. Therefore, it is of interest to examine, with nano-dynamic mechanical analysis (nano-DMA)[15], the complex modulus ($E*$) of resin-dentin interfaces submitted to load cycling. Even more, the complex modulus can be decomposed into storage (elastic) and loss (damping) of the modulus components[18]. The storage modulus E' (also called dynamic stiffness) characterizes the ability to store energy by the sample during a cycle of loading[16], which is then available for elastic recoil. The loss modulus characterizes the ability of the material to dissipate energy.

Thereby, it is required the capacity to absorb mechanical shock waves at these locations in order to prevent crack propagation across the boundary between the two phases of dentin[19]. DMA measures stiffness and damping; these are reported as modulus and tan delta. The ratio of the loss to the storage is the tan delta (δ). In this investigation, nano-DMA was used to evaluate mechanical behavior of human dentin, *i.e.,* the complex, storage and loss moduli, and tan (delta) for the underlying intertubular and peritubular dentin. Dental tissues are subjected to load cycling, due to the masticatory function, which considerably influences interactions between restorative materials and tooth tissues. Forces are transmitted to the bonded interface, which should support and dissipate this energy. Discrepancies in attained values of viscoelastic properties at the different structures within the dentin interface, mean a risk for cracking and breakdown of this interface, as low modulus regions lead to stress concentration in relatively high elastic modulus regions[20]. This may account for catastrophic failures of the restored teeth.

This study assessed the resin-dentin bond strength and the ability of an etch-and-rinse zinc-doped adhesive to induce an improvement of viscoelastic properties at the bonded carious dentin interface. This interface was created by using two different demineralization procedures on the caries-affected dentin surface, and after *in vitro* mechanical loading application. The study tested the two null hypotheses that, (1) bond strength and dynamic mechanical behavior, at the resin-caries affected dentin interface obtained with zinc-doped etch-and-rinse adhesives, is not influenced by different procedures of dentin conditioning, and (2) load cycling has no effect on the bond strength and dynamic mechanical behavior of samples bonded with zinc-doped adhesives to caries-affected dentin.

II. MATERIAL AND METHODS

A. Specimen preparation, bonding procedures and mechanical loading

Eighty-four human third molars with occlusal caries were obtained with informed consent from donors (20–40 year of age), under a protocol approved by the Institution Review Board (891/2014). Molars were stored at 4ºC in 0.5% chloramine T for up to 1 month before use. A flat mid-coronal carious dentin surface was exposed using a hard tissue microtome (Accutom-50; Struers, Copenhagen, Denmark) equipped with a slow-speed, water-cooled diamond wafering saw (330-CA RS-70300, Struers, Copenhagen, Denmark). The inclusion criteria for carious dentin were that the caries lesion, surrounded by sound dentin, should be limited to the occlusal surface, which extended at least half the distance from the enamel-dentin junction to the pulp chamber. To obtain caries-affected dentin, grinding was performed by applying the combined criteria of visual examination, surface hardness using a dental explorer, and staining by a caries detector solution (CDS, Kuraray Co., Ltd., Osaka, Japan). Using this procedure, all soft, stainable, carious dentin was removed. The relatively hard, caries-affected non staining dentin, on the experimental side was left[21]. A 180-grit silicon carbide (SiC) abrasive paper mounted on a water-cooled polishing machine (LaboPol-4, Struers, Copenhagen, Denmark) was used to produce a clinically relevant smear layer[22].

An etch-and-rinse adhesive system, Single Bond Plus (3M ESPE, St Paul, MN, USA) (SB), was tested. It was zinc doped by mixing the bonding resin with ZnO microparticles (average value particle size: 1 micron, Panreac Química, Barcelona, Spain) 20 wt% (SB-ZnO) or with 2 wt% $ZnCl_2$ (Sigma Aldrich, St Louis, MO, USA) (SB-ZnCl2). To achieve complete dissolution of $ZnCl_2$ and dispersion of ZnO nanoparticles, adhesive mixtures were vigorously shaken for 1 min in a tube agitator (Vortex Wizard, Ref. 51075; Velp Scientifica, Milan, Italy) before application. The complete process was performed in the dark. Adhesives containers were hermetically

closed during the procedure to assure that no solvent evaporation did occur. Employed chemical and adhesive descriptions are provided in Table I SI.

The specimens were divided into the following groups based on the tested adhesive systems and dentin-etching procedure: (i) SB was applied on 37% phosphoric acid (PA) treated dentin, 15 s (PA+SB); (ii) SB was applied on EDTA-treated dentin,0.5 M, 60 s (EDTA+SB); (iii) SB-ZnO was applied on 37% PA treated dentin; (iv) SB-ZnO was applied on EDTA-treated dentin, 0.5 M, 60 s; (v) SB-ZnCl$_2$ applied on 37% PA; (vi) SB-ZnCl$_2$ applied on EDTA-treated dentin, 0.5 M, 60 s.

The bonding procedures were performed in moist caries-affected dentin following the manufacturer′s instructions. A flowable resin composite (X-Flow, Dentsply, Caulk, UK) was placed incrementally in five 1 mm layers and light-cured with a Translux EC halogen unit (Kulzer GmbH, Bereich Dental, Wehrheim, Germany) for 40 s. Half of the carious teeth were stored for 24 h in simulated body fluid solution (SBF) and tested, while the other half were submitted to mechanical loading, in SBF. To proceed with the mechanical loading, specimens were mounted in a plastic rings using dental stone under 49 N (100,000 cycles, 3 cycles/seconds)[23], with a force that was exerted longitudinally along the center of the tooth. This compressive load was applied to the flat resin composite build-ups using a 5 mm diameter spherical stainless steel plunger that was attached to a cyclic loading machine (S-MMT-250NB; Shimadzu, Tokyo, Japan)[24]. The load cycling lasted 9 hours and 15 minutes and the loaded specimens were kept in SBF, at 37ºC until 24 h time completion. Restored carious teeth were sectioned into serial slabs, perpendicular to the bonded interface to produce bonded sections of approximately 1.0 mm thick. This yielded about three slabs of bonded caries-affected dentin *per* tooth. A total of 21 slabs were obtained from each experimental group.

B. Microtensile Bond Strength (MTBS)

Eighteen slabs from each experimental group were used for bond strength evaluation. Slabs were hand trimmed with a fine diamond bur into hourglass-shaped specimens, with the smallest dimension at the bonded interface ($1mm^2$). This trimming technique was chosen in order to accurately delimit the bonded tissue of interest (caries-affected dentin). Specimens were attached to a modified Bencor Multi-T testing apparatus (Danville Engineering Co., Danville, CA) with a cyanoacrylate adhesive (Zapit/Dental Venture of America Inc., Corona, CA, USA) and stressed to failure in tension (Instron 4411 /Instron Inc., Canton, MA, USA) at a crosshead speed of 0.5 mm/min. The cross-sectional area at the site of failure of the fractured specimens was measured to the nearest 0.01mm with a digital caliper (Sylvac Ultra-Call III, Fowler Co Inc., Newton, Mass, USA). Bond strength values were calculated in MPa. MTBS values were analyzed by two-way ANOVA (independent factors are mechanical loading and adhesive type) and Student Newman Keuls multiple comparisons tests. For all tests, statistical significance was set at $\alpha = 0.05$.

Fractured specimens were examined with a stereomicroscope (Olympus SZ-CTV, Olympus, Tokyo, Japan) at 40x magnification to determine the mode of failure. Failure modes were classified as adhesive or mixed. Representative specimens of each group were maintained for 48 h in a desiccator (Sample Dry Keeper Simulate Corp., Osaka, Japan), mounted on aluminum stubs with carbon cement and carbon sputter-coated (Unit E500, Polaron Equipment Ltd., Watford, England). Prepared specimens were observed with field emission scanning electron microscopy (FESEM) (FESEM Gemini, Carl Zeiss, Oberkochen, Germany) at an accelerating voltage of 3 kV, in order to evaluate the morphology of the debonded interfaces. Energy-dispersive analysis was

performed in selected points using an X-ray detector system (EDX Inca 300, Oxford Instruments, Oxford, UK) attached to the FESEM.

C. Nano-DMA analysis and Atomic Force Microscopy (AFM) imaging

Three slabs of restored carious teeth were submitted to nano-DMA and AFM analysis. Bonded interphases were polished with SiC abrasive paper from 800 up to 4.000-grit with a final polishing procedure performed with diamond pastes (Buehler-MetaDi, Buehler Ltd Illinois, USA), through 1 μm down to 0.25 μm. The specimens were treated in an ultrasonic bath (Model QS3, Ultrawave Ltd, Cardiff, UK) containing deionized water [pH 7.4] for 5 min at each polishing step. Property mappings were conducted using a Ti-750D TriboIndenter (Hysitron, Inc., Minneapolis, MN) equipped with nano-DMA III, a commercial nano-DMA package. The nanoindenter (Berkovich tip; tip radius $\sim$20 nm) was calibrated against a fused quartz sample using a quasistatic force setpoint of 5 μN to maintain contact between the tip and the sample surface. A dynamic oscillating force of 5 μN was superimposed on the quasistatic signal at a frequency of 200 Hz. Based on a calibration modulus of the tip value of 69.6 GPa for the fused quartz, the best-fit spherical radius approximation for the tip was 150 nm, for the selected nano-DMA scanning parameters. After calibrating, modulus mapping of the samples was conducted by imposing a quasistatic force setpoint, F_q =5 μN, to which a sinusoidal force of amplitude F_A=1.8 μN and frequency f=200 Hz was superimposed. Data from regions approximately 30x30 μm in size were collected using a scan rate of 0.2 Hz. Each scan resulted in a 256 x 256 pixel data array. Specimens were scanned in the hydrated condition by the application of a layer of ethylene glycol over the specimen surface to prevent water evaporation during the analysis. Viscoelastic data were acquired on the three different specimens and obtained from selected surface areas of the substrate using a rastering scan pattern. For each property map, 10 sets of 225

datapoints were used to obtain the mean value of a particular region of interest. That is, the 225 datapoints represent 1.47 x 1.47 = 2.15 μm^2 of each 30 x 30 = 900 μm^2 of the scan. The datapoints from 10 such non-overlapping squares were obtained for each zone at the bonded interface; thus, for each nano-DMA parameter, 30 values (3 specimens x 10 squares) were generated in each zone: hybrid layer (HL), bottom of hybrid layer (BHL), intertubular dentin (ID) and peritubular dentin (PD) (Figure 1).
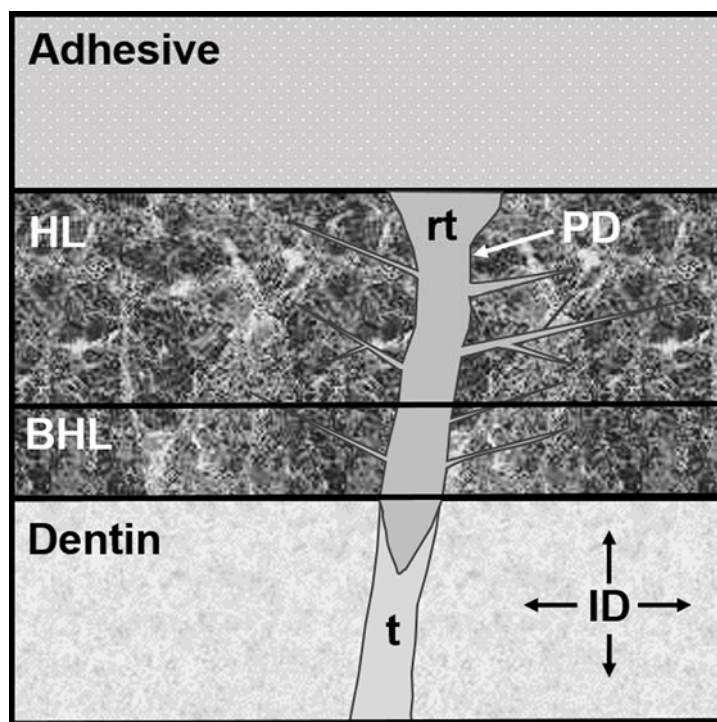
Figure 1. Schematic illustration of the resin-dentin interface to be indented. HL, hybrid layer; BHL, bottom of hybrid layer; PD, peritubular dentin; ID, intertubular dentin; rt, resin tag; t, dentinal tubule.

Under steady conditions (application of a quasistatic force) the indentation modulus of the tested sample (*E)* was obtained by application of different models that relate the indentation force (*F*) and depth (*D*). Most of these theories assume proportionality between the force and the indentation modulus[25-27]. Statistical analyses were performed

with ANOVA and Student Newman Keuls multiple comparisons tests. P<0.05 was set for significance.

An atomic force microscope (AFM Nanoscope V, Digital Instruments, Veeco Metrology group, Santa Barbara, CA, USA) equipped with a Triboscope indentor system (Hysitron Inc., Minneapolis, MN) was employed in this study for topography mappings. The imaging process was undertaken inside a wet cell in a fully hydrated state, using the tapping mode, with a calibrated vertical-engaged piezo-scanner (Digital Instrument, Santa Barbara, CA, USA). A 10 nm radius silicon nitride tip (Veeco) was attached to the end of an oscillating cantilever that came into intermittent contact with the surface at the lowest point of the oscillation. Changes in vertical position of the AFM tip at resonance frequencies near 330 kHz provided the height of the images registered as bright and dark regions. 50 x 50 μm digital images were recorded from each bonded interface, with a slow scan rate (0.1 Hz).

A graphical abstract representing the schematics and the central premise of the paper is shown at the Figure 2.
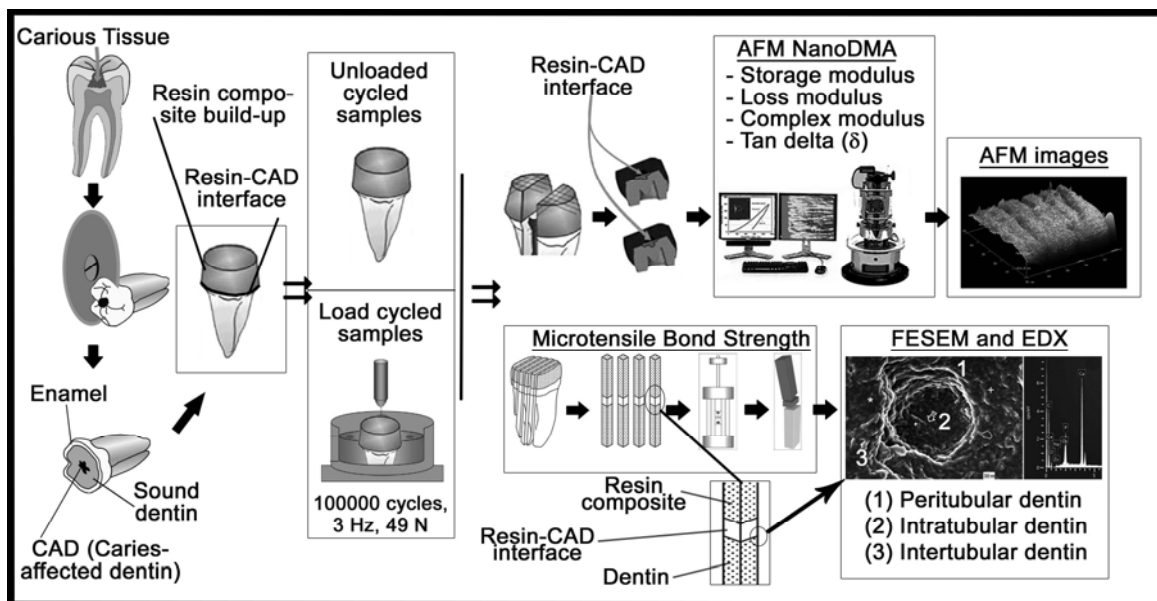
Figure 2. Description of the structure and the central premise of the research.

III. RESULTS AND DISCUSSION

Scanning mode nano-DMA analysis of the map of the viscoelastic properties attained at the resin-carious dentin interface is depicted in Figures 3 to 5. FESEM images and EDX spectra are provided in Figure 6. Topographic mapping from AFM images are included in Figure 7. A flowchart of procedures and outcomes has been included in Figure 8. Table I represents mean and standard deviation of the microtensile bond strength (MTBS).
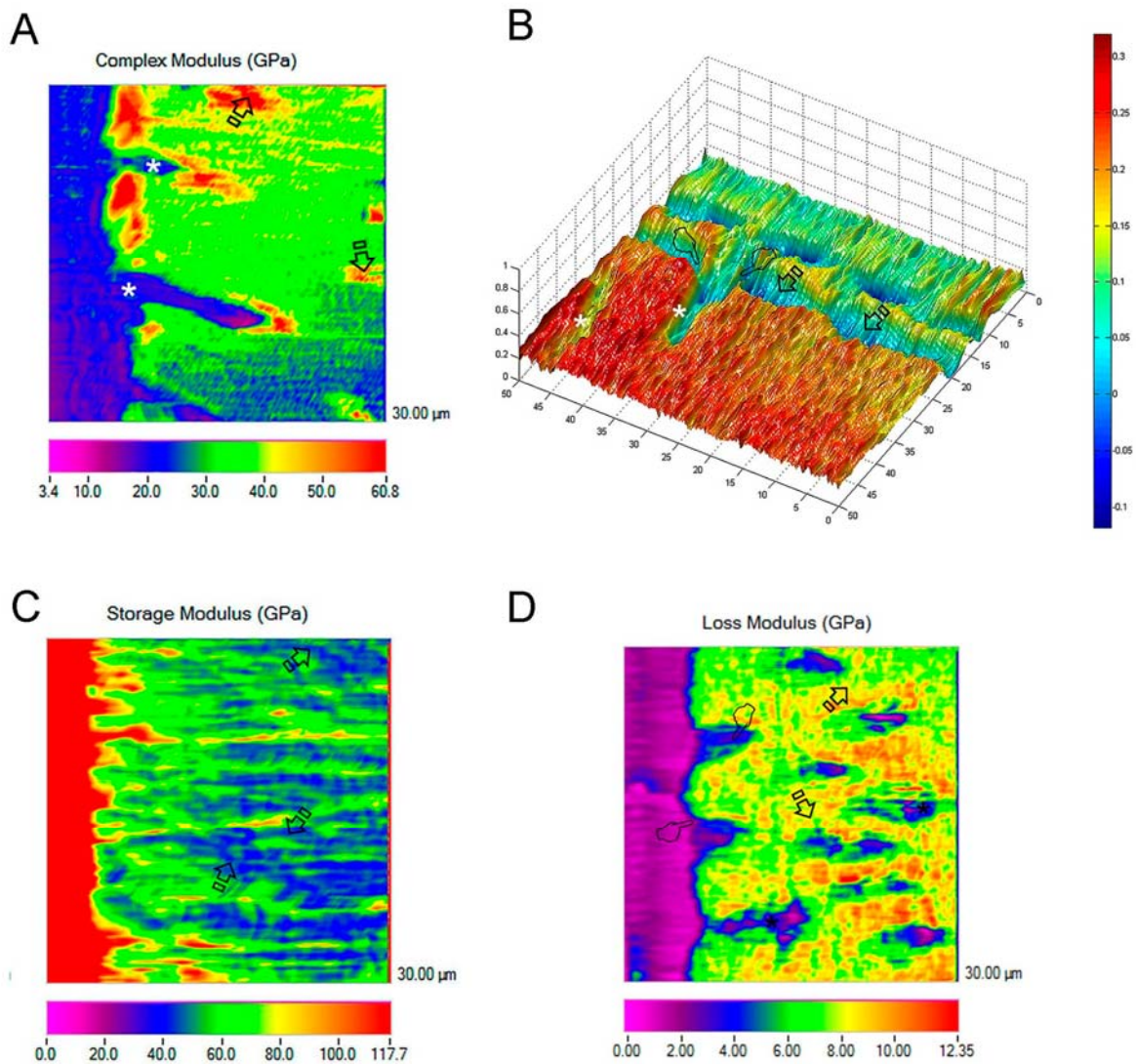
Figure 3. A, Scanning mode nano-DMA analysis of the complex modulus/E^* at the PA+SB-caries-affected dentin interface, load cycled. In the color scheme shown, the

redder color corresponds to higher values of the locally measured moduli. It is reflected some discontinuous red envelops of high complex modulus (arrows), and limited areas of low values, in blue (asterisks). **B**, 3-D contour map of the tan δ distribution in a specimen of carious dentin treated with PA+SB-ZnCl$_2$, load cycled. At the resin-dentin inter-diffusion zone, tan δ ranged from 0.03 (bottom of hybrid layer) to 0.17 (hybrid layer), creating a zone of lower dissipation of energy, and thereby promoting stress concentration and breaking with failure of the resin-dentin interface (arrows). Magnitudes of X, Y and Z axis are in microns. **C,** Scanning mode nano-DMA analysis of the map of the storage modulus/E' at the EDTA+SB-caries-affected dentin interface, load cycled. The lowest E' was attained at peritubular dentin, where the presence of clear blue regions is significant (B) (arrows). **D,** Scanning mode nano-DMA analysis of the map of the loss modulus/E'', at the EDTA+SB-ZnCl$_2$ caries-affected dentin interface, load cycled. Large extension of higher loss moduli values (arrows) were observed at peritubular dentin (yellow) (B), in contrast with the hybrid layer (pointer) and the bottom of the hybrid layer (asterisks), which showed the lowest values, 1.48 and 1.14 GPa, respectively.
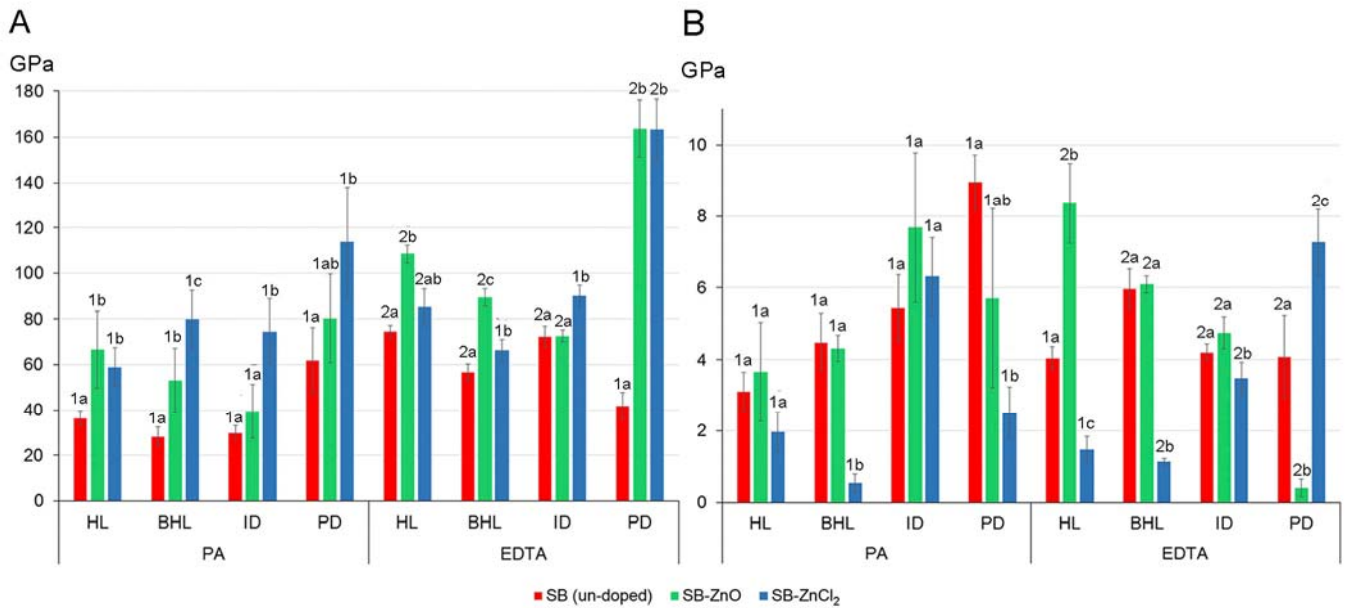
Figure 4: Mean and standard deviation of storage modulus (GPa) (A), and loss modulus (GPa) (B) at experimental adhesive resin-carious dentin interfaces, load cycled. Same lower case letters indicate no differences among adhesives and same numbers indicate no differences between PA and EDTA groups. Student Neuman Keuls ($p < 0.05$). Abbreviations: PA: Phosphoric acid, EDTA: ethylenediaminetetraacetic acid, SB: Single Bond, HL: Hybrid Layer, BHL: Bottom of Hybrid Layer, ID: Intertubular Dentin, PD: Peritubular Dentin, SB: Single Bond adhesive, SB-ZnO: adhesive doped with zinc oxide, SB-ZnCl$_2$: adhesive doped with zinc chloride.
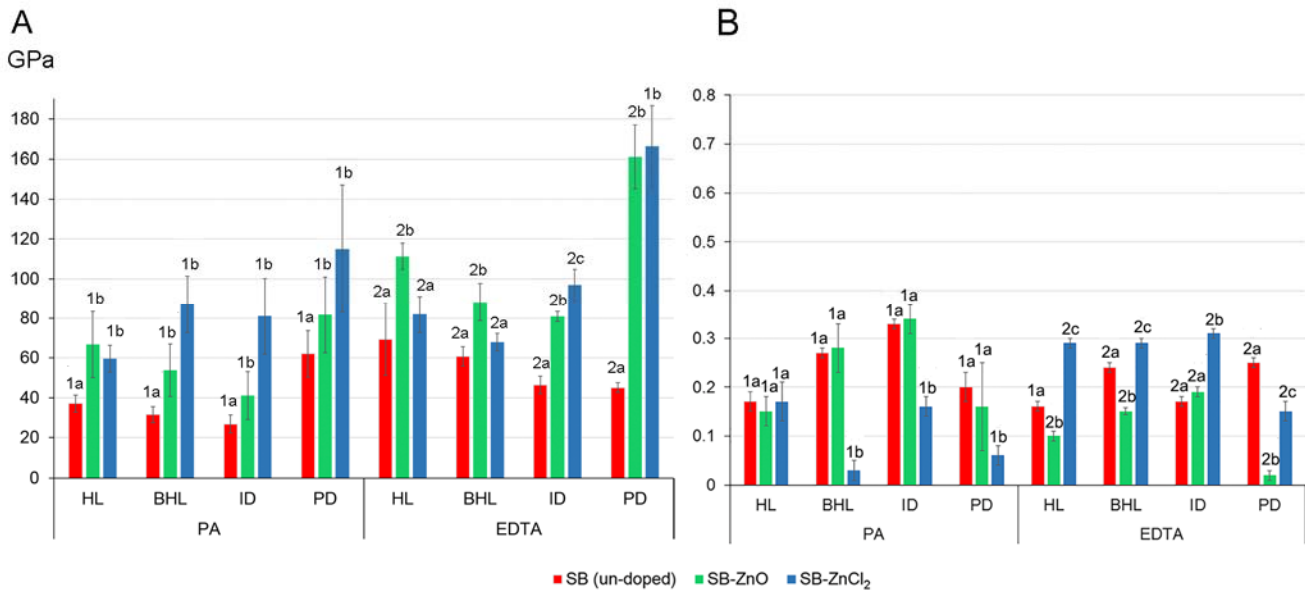
Figure 5: Mean and standard deviation of complex modulus (GPa) (A) and tan δ (B) at the experimental adhesive resin-carious dentin interfaces, load cycled. Same lower case letters indicate no differences among adhesives and same numbers indicate no differences between PA and EDTA groups. Student Neuman Keuls (p<0.05). Abbreviations: PA: Phosphoric acid, EDTA: ethylenediaminetetraacetic acid, SB: Single Bond, HL: Hybrid Layer, BHL: Bottom of Hybrid Layer, ID: Intertubular Dentin, PD: Peritubular Dentin, SB: Single Bond adhesive, SB-ZnO: adhesive doped with zinc oxide, SB-ZnCl₂: adhesive doped with zinc chloride.
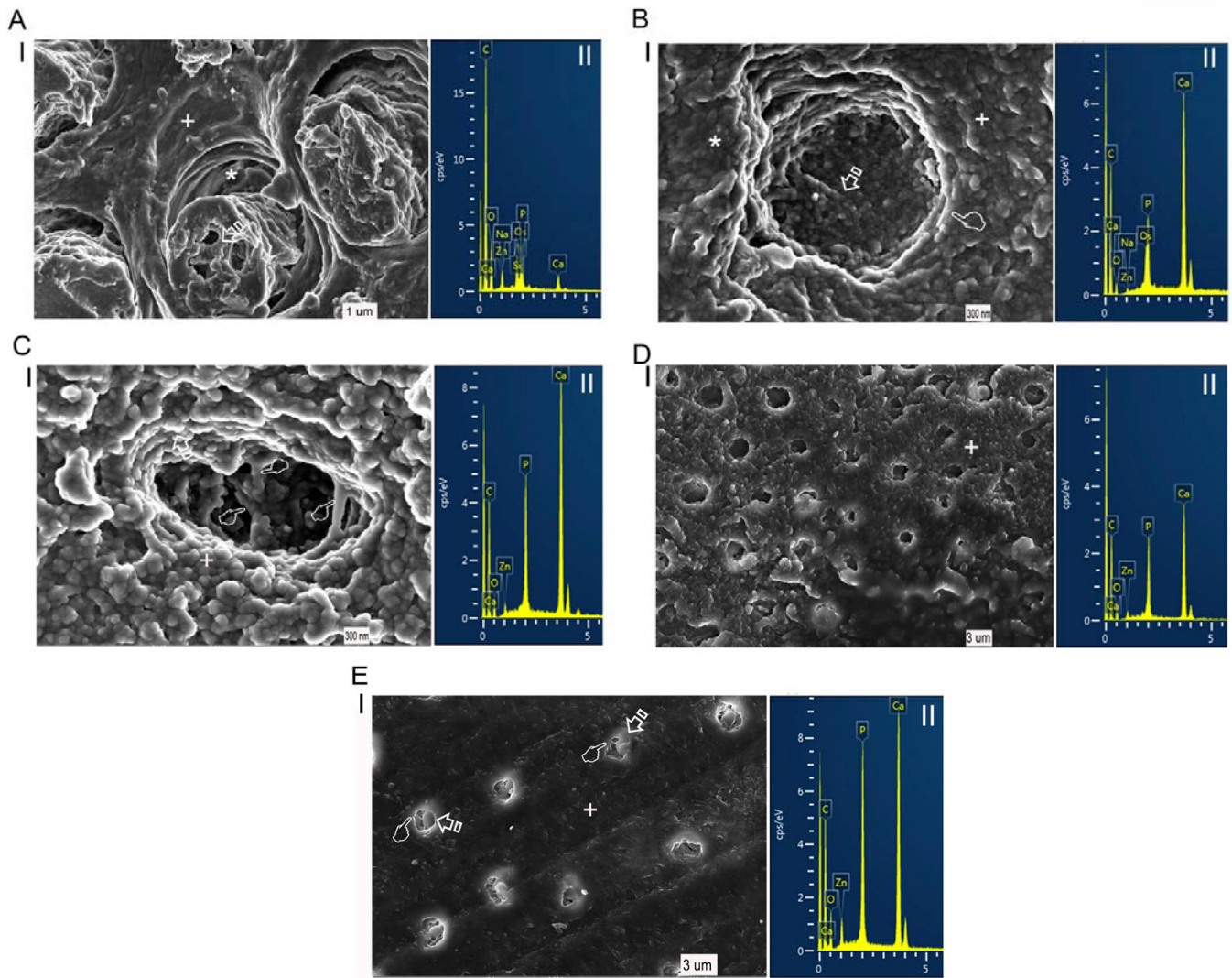
Figure 6: Field emission scanning electron microscopy (FESEM) images of failures after bonding and MTBS testing. (A) PA+SB-ZnO unloaded. (B) PA+SB-ZnO load cycled. (C) PA+SB-ZnCl$_2$ load cycled. (D) EDTA+SB-ZnO load cycled. (E) EDTA+SB-ZnCl$_2$ load cycled. Spectra from energy dispersive (EDX) analysis show elemental compositions of phosphorus (P), calcium (Ca), and zinc (Zn) in all images (·II). + indicates the points where the elemental analysis spectra were taken.
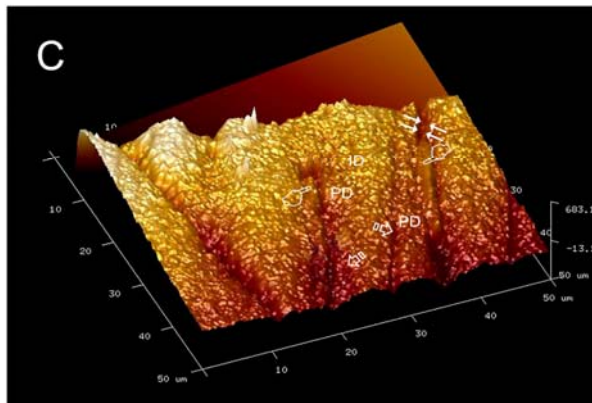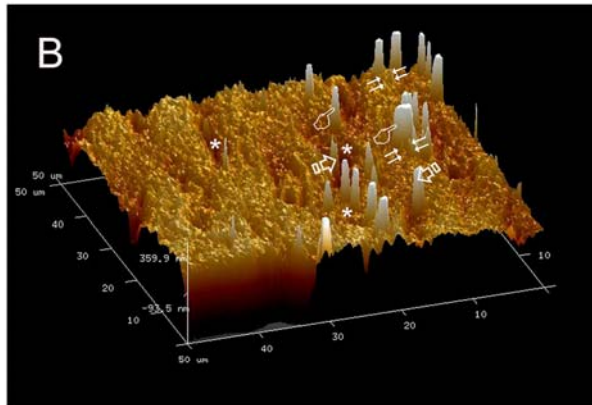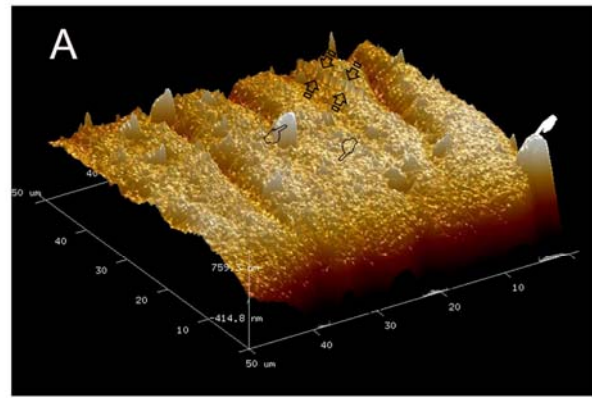
Figure 7. Topography mappings of resin infiltrated carious dentin obtained by AFM after applying PA+SB-ZnO (A), EDTA+SB-ZnO (B) or EDTA+SB-ZnCl$_2$ (C), and load cycled.
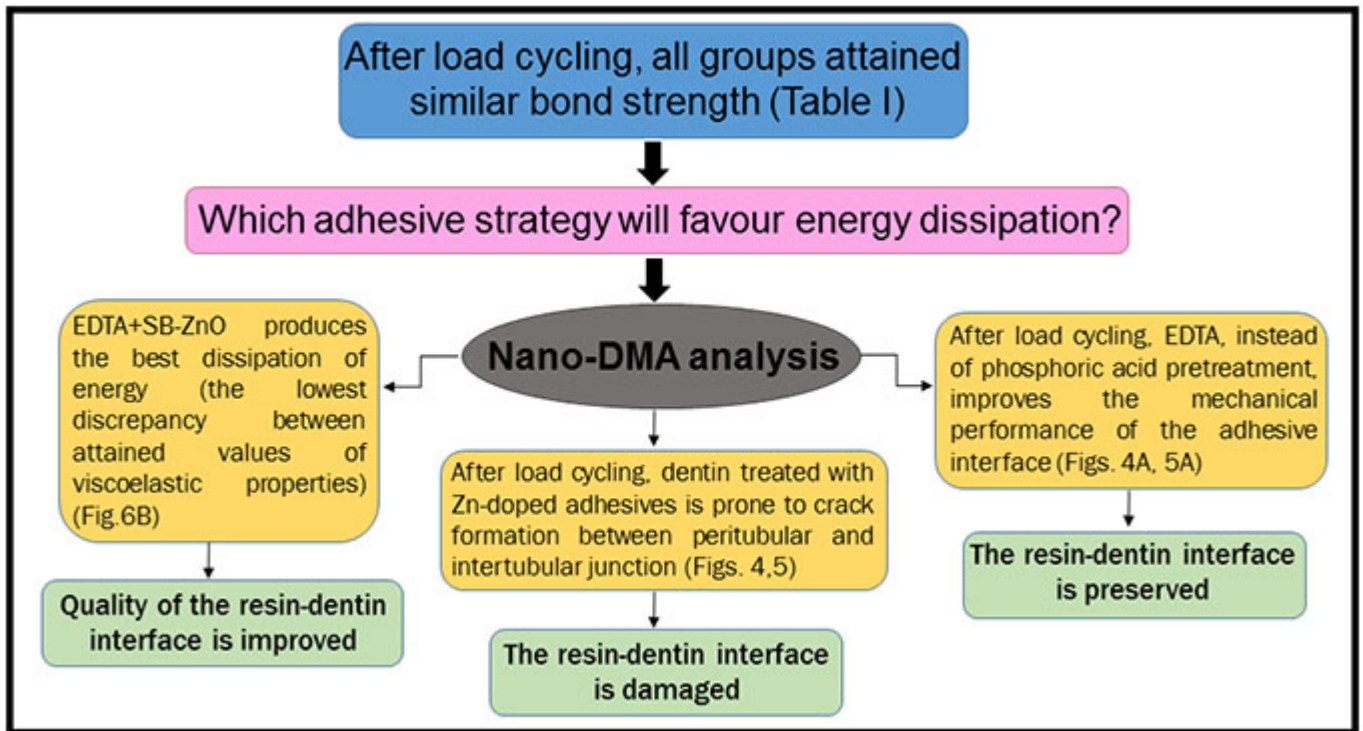
Figure 8: Flowchart showing the main findings obtained in this study.

Table I. Mean and standard deviation of microtensile bond strength values (MPa), and percentage distribution (%) of failure mode (A: Adhesive; M: Mixed), obtained for the different experimental groups.

	UNLOADED			LOADED		
	Mean (SD) MPa	A %	M %	Mean (SD) MPa	A %	M %
PA+SB	23.49 (2.99) A1	24	76	20.96 (3.36) a1	68	32
PA+SB-ZnO	17.73 (2.33) B1	47	53	16.86 (3.77) a1	53	47
PA+SB-ZnCl$_2$	15.88 (2.03) B1	58	42	17.75 (4.45) a1	68	32
EDTA+SB	21.75 (2.34) A1	33	67	21.28 (3.70) a1	55	45
EDTA+SB-ZnO	15.05 (3.05) B1	39	61	15.52 (3.55) a1	52	48
EDTA+SB-ZnCl$_2$	19.46 (3.21) AB1	31	69	22.26 (3.66) a1	71	29

Abbreviations: EDTA: ethylenediaminetetraacetic acid; PA: phosphoric acid; SB: Single-Bond.
Identical letters indicate no significant difference in columns and numbers in rows, after Student-Newman-Keuls or Student t tests ($p < 0.05$).

The present results confirm that load cycling of caries-affected dentin surfaces conditioned with phosphoric acid or EDTA, and infiltrated with an etch-and-rinse adhesive doped with zinc oxide or zinc chloride influenced the dynamic mechanical behavior at the resin/caries-affected dentin interface. The most favorable dissipation of energy through the resin/caries-affected dentin interface occurs when EDTA is used to pretreat the dentin and the etch-and-rinse adhesive is ZnO-doped. At these interfaces, very low discrepancies were found between the attained values of viscoelastic properties at the different dentin structures. It accounts for a favorable stress dissipation at the bonded interface, lowering the risk for cracking and breakdown (Misra et al., 2004). Therefore, homogeneous values of viscoelastic properties facilitates the masticatory forces transmission through the different zones at the resin dentin interface.

Load cycling did not affect bond strength in any group, but contributed to increase the percentage of adhesive over mixed failures (Table I). The effect of load cycling in dentin bonding efficacy, had controversial results throughout the dental literature. In general terms, a decrease in bonding efficacy after using Single Bond has been previously reported after mechanical loading[24]. It was pointed out that fatigue stress[28] produces a failure mostly at the top or beneath the HL where demineralized collagen fibrils were exposed and the adhesive failed to envelop the collagen network properly [24,29]. The increase in the percentage of adhesive failures may be interpreted as a result after the strengthening of the resin-dentin interface from remineralization[30]. Specimens of resin-bonded caries-affected dentin usually failed cohesively within dentin, presumably because it was weaker than the bonding interface[31]. Therefore, the second null hypothesis which reads "load cycling has no effect on the bond strength and dynamic mechanical behavior of samples bonded with zinc-doped adhesives to caries-affected dentin", was accepted.

The first null hypothesis, "bond strength and dynamic mechanical behavior, at the resin-caries affected dentin interface obtained with zinc-doped etch-and-rinse adhesives, is not influenced by different procedures of dentin conditioning", must be rejected, as storage or elastic modulus augmented in dentin treated with PA+SB, at HL (~1.70 fold), BHL (~1.55 fold), ID (~1.78 fold) and PT (~2.59 fold), respectively, when specimens were load cycled (Fig. 4A). Low storage modulus (E') regions with high flexibility (*e.g*, ID: 29.98 GPa) lead to stress concentration in relatively high elastic modulus regions, with low flexibility[32].Thus, the energy stored would potentially be dissipated through cracking the tissue[20], *i.e.*, the resin-carious dentin interface. Increased mineralization was also observed when specimens treated with PA+SB-ZnO were submitted to mechanical loading, as microstructural analysis unveils mineral deposits within the lumen of tubules, after mechanical stimulation (Fig. 6B) (arrow). In this group, minerals formed a collar around the tubule lumen (pointer), detected below a platform of crystals (asterisk). If the bond between the adhesive tags and peritubular dentin is imperfect even though remineralized, as in Fig. 6A·I (asterisk), then the stress concentration zones are probably within the hybrid layer and bottom of the hybrid layer[20]. Within tubular structures, energy dissipation can occur via deformation in axial and radial directions[33], as validated from the AFM images. These figures show some stick-slip images, in radial direction, of nucleated minerals resulted observable at the resin-infiltrated intertubular dentin, as sign of energy dissipation (Fig. 7A), (faced double arrows).

Samples treated with EDTA+SB and load cycled attained a significant lower value of the storage moduli at the peritubular dentin. Clear blue traces signaled those regions of lower resistance to deformation and elastic energy stored, respectively, when observed at the scanning mode nano-DMA analysis (Fig 3C). This lower value of viscoelastic performance resulted associated with layered minerals which precipitated,

preferentially, at intertubular dentin forming a consistent clump of crystals. These crystals were deposited in *strata* at the intertubular dentin, and the tubules remained empty when ZnO was used for doping (Fig. 6D). When samples treated with EDTA+SB-ZnO were submitted to load cycling, some bridge and rod-like new mineral formations were observed surrounding the intratubular crystals (faced double arrows). These crystals precipitated anchored the intratubular deposits of mineral to the peritubular dentin reducing the tubule entrances (asterisks) (Fig 7B). On the other hand, tubules appeared with intratubular mineral deposits formed of zinc and calcium phosphate salts when $ZnCl_2$ was selected (Figs. 6E·I, 6E·II). When specimens were treated with EDTA+SB-$ZnCl_2$ and then load cycled, new mineral formations were observed as multiple rod-like figures surrounding the intratubular crystals (Figs. 6E·I, 7C). These mineral beams remained anchored, directly or indirectly through crack-bridging or bridging-like structures, sticking the intratubular deposits of mineral to the peritubular dentin. These samples showed some breakdown zones (Fig. 7C) (arrows) at the interface, located at the limits between the peritubular (PD) and intertubular dentin (ID), being parallel to the intratubular mineral deposits.

The loss modulus characterizes the viscous behavior[34], and is a measure of the energy lost as it represents the dampening capacity of a material[35]. Dissipation of energy within the structures is of prime importance in dynamic systems[33] such as the oral environment. Loss moduli performed similarly among the specimens treated with PA+SB, regardless the presence of zinc, when they were not load cycled. Samples conditioned with phosphoric acid and infiltrated with SB-ZnO obtained the least discrepancy between values of loss moduli among the phosphoric acid conditioned specimens after loading. Similar values of loss moduli within the bonded layers will preserve the integrity of the resin-dentin interface against cracking and failure (Fig. 6B).

Processes of intertubular and intratubular mineralization are taken place at these interfaces (pointers) (Fig 7A). In general, loss moduli is lower after using PA+SB-ZnCl$_2$, in comparison with the unloaded group, then dentin is prone to fracture[36]. Some tubules appeared partially occluded, but with mineralized peritubular dentin (arrow) and some "bridging" processes (pointers) (Fig. 6C). ZnCl$_2$ is highly acidic,[37] soluble, and hydrophilic. When it is added to the adhesive blend, may produce an over-etching effect within the infiltrated dentin, demineralizing the underlying dentin[17,35]. These findings comply with the lowest bond strength values that were attained, and the high percentage of adhesive failures at the interface (Table I).

When EDTA was used to pre-treat the dentin surface, in general, loss moduli was not affected after loading those specimens that were infiltrated with SB or with SB-ZnO (Fig. 4B). On the contrary, samples treated with EDTA+SB-ZnCl$_2$ attained lower loss moduli after load cycling, *i.e*, lower amount of energy lost[35], except at the peritubular dentin, where it significantly increased (Fig. 3D). Occurrence of adhesive failures at the bonded interface will permit to observe little rod-like new minerals surrounding the intratubular crystals, directly (arrows) or indirectly (pointers) anchored on the intratubular deposits of mineral to the peritubular dentin (Fig 6E·I), through calcium phosphate Zn-based salts formation (Fig 6E·I). Samples treated with EDTA and infiltrated with SB-ZnCl$_2$ achieved a higher discrepancy between values of loss modulus than the un-doped group, hindering the right dissipation of energy. Those outcomes may be due to the thinner layer of demineralized dentin created by EDTA treatment. Although such thin layers of demineralized dentin may be easier to infiltrate with resin adhesives[38], they may create higher stress concentration under cyclic loading. Apparently, this results improbable in PA-etched dentin that produces a deeper

demineralized layer which may distribute stresses over a greater volume of collagen, thereby lowering stress concentrations[39].

The resistance to dynamic deformation or robustness is given by the value of the complex modulus. Load cycling promoted an increase of the complex modulus (E^*) at the hybrid layer (HL) (~1.52 fold), bottom of hybrid layer (BHL) (~1.74 fold), intertubular dentin (ID) (~1.49 fold) and peritubular dentin (PD) (~2.38 fold) in the un-doped specimens of PA+SB (Fig. 5A). The significance of this finding lies in the major resistance to deformation that is achieved at the whole resin-dentin interface (Figure 1A). Scanning of interfaces enabled identification of both peritubular and intertubular dentin in the property maps as one of the most crucial junctions for preventing crack generation and propagation across the boundary between the two different phases[40]. When specimens were treated with phosphoric acid and Single Bond (PA+SB) and then load cycled, the complex moduli at peritubular and intertubular dentin attained the highest values (62.01 and 29.98 GPa, respectively) among all tests. Numerical data permit association of the red and yellow colors with the viscoelastic behavior of both peritubular and intertubular dentin, respectively (Figs. 3A, 5A). The present complex moduli, in the unloaded group are within the range previously published by Kinney et al. (1999)[41] and Katz et al. (2001)[42], who reported 26-30 GPa and 13-20 GPa for peritubular and intertubular sound dentin, respectively. Ryou et al. (2015)[43] obtained an average complex modulus of old intertubular and peritubular dentin of ~21 and 31 GPa. The discrepancy between the outcomes that were obtained are due to the fact that their measurements were performed in dry conditions[36] and at non-carious dentin.

Samples (unloaded and loaded) treated with EDTA+SB increased their complex moduli and, thereby, their remineralization[44] in comparison with teeth treated with PA+SB. Thereby, it is shown higher resistance to deformation but with a low range of numerical

values amongst the four constituents of the interface (Fig 2A SI). When $ZnCl_2$ was used as a doping agent, little rod-like new mineral (faced double arrows), as bridge-like structures, anchored the intratubular crystals to the peritubular wall. The nano-DMA mapping analysis of peritubular dentin (Fig. 3D) permitted observation of zones with high complex modulus close to areas of low modulus. These areas might hinder the dissipation of energy through the tested interface[33].

Tan δ decreased at both hybrid layer and intertubular dentin, after load cycling, when specimens were treated with phosphoric acid and Single Bond (PA+SB) (Figs. 1 SI, 5B). Tan δ reflects how a material can get rid of the energy. The lower tan δ, the greater the proportion of energy available in the system for recoil and/or failure[34]. Tan δ was not affected after loading carious dentin treated with EDTA+SB, except at the bottom of the hybrid layer and peritubular dentin, where it was increased ~1.33 and 3.47 fold, respectively (Fig. 5B). As a consequence, a general trend to rise levels of accumulated energies can be appreciated when those dentin samples are pre-treated with EDTA, and load cycled. This tendency was not observed at the unloaded samples (Fig 2B SI). Load cycled specimens treated with PA+SB-$ZnCl_2$ increased tan δ, in general, when compared with the un-doped group (Figs. 5B, 5 SI B). As a result, the combination of factors such as mechanical stimuli and presence of zinc-chloride into the chemical formulation of the adhesive resin served as leverage effects of stored energy at the interface. High differences between values of tan δ were attained between intertubular (0.16) and peritubular dentin (0.06), contributing to the generalized breakdown of the interface (pointers). Failure and fracture was also located between the bottom of the hybrid layer (0.03) and the intertubular dentin (0.16) (asterisks), where stresses and energies were concentrated and accumulated (Fig. 3B). A general decrease of tan δ was observed after load cycling when ZnO was used (Fig. 4 SI), and an increase

at the whole structure of the interface after using $ZnCl_2$ was determined, in comparison with the control group (EDTA+SB) (Fig.5B).

Zn-doped adhesives and load cycling have contributed to the remineralization of resin-dentin interfaces, based on the increased static nano-mechanical properties and the enhanced biochemical markers at both mineral and collagen of the dentin substrate[45,46]. Nevertheless, the biomechanical significance of the results that were obtained in the present study complies with resin-dentin interfaces that facilitate the energy loss. Thus, it results in a lower proportion of energy available for failure or recoil when carious dentin is pretreated with EDTA, and the SB-$ZnCl_2$ doped adhesive is employed to restore carious dentin, that will be subjected to mechanical function (Fig.8).

These are to the best of our knowledge, the only available results from nano-DMA experiments on Zn-doped infiltrated-resin in carious dentin. Nevertheless, a complementary study of nanomechanical properties based on both hardness and static Young modulus, aimed to determine functional remineralization, would probably have contributed to expand the significance and applicability of these results. Future research should also be aimed to physico-chemically characterize these resin-carious dentin interfaces through micro-Raman and cluster analysis, micro-XRD[2] and TEM studies. Additional microscopic techniques, as Masson's trichrome staining and dye assisted confocal microscopy evaluation (CLSM) would also help to understand the changes that are promoted at this location.

IV. CONCLUSIONS

A. After load cycling, the higher proportion of energy available at the resin-dentin interface appeared at the peritubular dentin when EDTA+SB-ZnO and PA+SB-$ZnCl_2$ were used, and at the bottom of the hybrid layer when PA+SB-$ZnCl_2$ was employed. From this approach, EDTA+SB-ZnO represents the adhesive

technique that will better favor the dissipation of energy through the resin/caries-affected dentin interface.

B. Viscoelastic properties of carious dentin infiltrated with Zn-based compounds and load cycled, attained higher discrepancy between values at intertubular and peritubular dentin, posing a potential risk for cracking and breakdown of the tissue at this level.

C. Discrepancies of both complex and storage moduli between intertubular and peritubular dentin were higher when phosphoric acid was used to pretreat the carious dentin, instead of EDTA, if using non doped resins in samples submitted to mechanical loading. Thereby, EDTA conditioning may contribute to enhance the long-term behavior of resin-carious dentin interfaces.

D. Carious dentin was prone to fracture when samples were infiltrated with SB-$ZnCl_2$, regardless of EDTA or phosphoric acid etching, as loss moduli decreased at the resin-dentin interface, after load cycling. This adhesive procedure should be discouraged.

REFERENCES

[1]J.H. Kinney, S.J. Marshall, and G.W. Marshall, Crit. Rev. Oral Biol. Med. **14**, 13 (2003).

[2]L.E. Bertassoni, S. Habelitz, J.H. Kinney, S.J. Marshall, and G.W. Marshall, Caries Res. **43**, 70 (2009).

[3]J. De Munck, K. Van Landuyt, M. Peumans, A. Poitevin, P. Lambrechts, M. Braem, and B. Van Meerbeek, J. Dent. Res. **84**, 118 (2005).

[4]Y. Wang, P. Spencer, and M.P. Walker, J. Biomed. Mater. Res. A **81**, 279 (2007).

[5]H.A. Wege, J.A. Aguilar, M.A. Rodríguez-Valverde, M. Toledano, R. Osorio, and M.A. Cabrerizo-Vílchez, J. Colloid Interface Sci. **263**, 162 (2003).

[6]R. Osorio, M. Yamauti, E. Osorio, M.E. Ruiz-Requena, D. Pashley, F. Tay, and M. Toledano, Eur J. Oral Sci. **119**, 79 (2011).

[7]M. Toledano, E. Osorio, F.S. Aguilera, S. Sauro, I. Cabello, and R. Osorio, J. Mech. Behav. Biomed. Mater. **30**, 61 (2014).

[8]P. Spencer and Y. Wang, J. Dent. Res. **80**, 1400 (2001).

[9]Y. Liu, S. Mai, N. Li, C.K. Yiu, J. Mao, D.H. Pashley, and F.R. Tay, Acta Biomater. **7**, 1742 (2011).

[10]T. Takatsuka, K. Tanaka, and Y. Iijima, Dent. Mater. **21,** 1170 (2005).

[11]M. Toledano, S. Sauro, I. Cabello, T. Watson, and R. Osorio, Dent. Mater. **29**, e142 (2013).

[12]Z. Yang and C. Xie, Colloids Surf. B. Biointerfaces **47**, 140 (2006).

[13]J. Pasquet, Y. Chevalier, J. Pelletier, E. Couval, D. Bouvier, and M. Bolzinger, Colloids and Surfaces A: Physicochem. Eng. Aspects. **457**, 263 (2014).

[14]R. Osorio, M. Yamauti, E. Osorio, J.S. Román, and M. Toledano, Eur. J. Oral Sci. **119**, 401 (2011).

[15]M. Toledano, F.S. Aguilera, E. Osorio, M.T. López-López, I. Cabello, M. Toledano-Osorio, and R. Osorio, Biointerphases **10,** 041004 (2015).

[16]C.M. Hayot, E. Forouzesh, A. Goel, Z. Avramova, and J.A. Turner, J. Exp. Bot. **63**, 2525 (2012).

[17]M.A. Meyers and K.K. Chawla, Mechanical behavior of materials, Prentice-Hall, New Jersey, USA, 1999), pp. 98,103.

[18]T.M. Wilkinson, S. Zargari, M. Prasad, and C.E. Packard, J. Mater. Sci. **50**, 1041 (2015).

[19]G.W. Marshall, S. Habelitz, R. Gallagher, M. Balooch, G. Balooch, and S.J. Marshall, J. Dent. Res. **80**, 1768 (2001).

[20]A. Misra, P. Spencer, O. Marangos, Y. Wang, and J.L. Katz, J. Biomed. Mater. Res. B: Appl. Biomater. **70**, 56 (2004).

[21]M.C. Erhardt, M. Toledano, R. Osorio, and L.A. Pimenta, Dent. Mater. 24, 786 (2008).

[22]H. Koibuchi, N. Yasuda, and N. Nakabayashi, Dent. Mater. **17**, 122 (2001).

[23]M. Toledano, F.S. Aguilera, I. Cabello, and R. Osorio, Biomech. Model. Mechanobiol. **13**, 1289 (2014).

[24]M. Toledano, R. Osorio, A. Albaladejo, F.S. Aguilera, F.R. Tay, and M. Ferrari, Oper. Dent. **31**, 25 (2006).

[25]L. Han, A.J. Grodzinsky, and C. Ortiz, Annu. Rev. Mater. Res. **41**, 133 (2011).

[26]H. Hertz, J. R. Angew. Math. **92**, 156 (1881).

[27]W.C. Oliver and G.M. Pharr, J. Mater. Res. **7**, 1564 (1992).

[28]T. Nikaido, K.H. Kunzelmann, H. Chen, M. Ogata, N. Harada, S. Yamaguchi, C.F. Cox, R. Hickel, and J. Tagami, Dent. Mater. **18**, 269 (2002).

[29]C. Prati, S. Chersoni, and D.H. Pashley, Dent. Mater. **15**, 323 (1999).

[30]M. Toledano, E. Osorio, I. Cabello, F.S. Aguilera, M.T. López-López, M. Toledano-Osorio, and R. Osorio, J. Mech. Behav. Biomed. Mater. **54**, 33 (2016).

[31]M. Toledano, I. Cabello, M. Yamauti, and R. Osorio, Microsc. Microanal. **18**, 497 (2012).

[32]V. Gopalakrishnan and C.F. Zukoski, J. Rheol. **51**, 623 (2007).

[33]R. Agrawal, A. Nieto, H. Chen, M. Mora, and A. Agarwal, ACS Appl. Mater. Interfaces 27, 12052 (2013).

[34]D.M. Espino, D.E.T. Shepherd, and D.W.L. Hukins, BMC Musculoskelet. Disord. **15**, 205 (2014).

[35]M.L. Lee, Y. Li, Y.P. Feng, and C.W. Carter, Intermetallics **10**, 1061 (2002).

[36]G. Balooch, G.W. Marshall, S.J. Marshall, O.L. Warren, S.A. Asif, and M. Balooch, J. Biomech. **37**, 1223 (2004).

[37]I.D. Brown, The chemical bond in inorganic chemistry: the bond valence model, (Oxford University Press, Oxford, 2006).

[38]K.L. Van Landuyt, Y. Yoshida, I. Hirata, J. Snauwaert, J. De Munck, M. Okazaki, K. Suzuki, P. Lambrechts, and B. Van Meerbeek, J. Dent. Res. **87**, 757 (2008).

[39]S. Sauro, M. Toledano, F.S. Aguilera, F. Mannocci, D.H. Pashley, F.R. Tay, T.F. Watson, and R. Osorio, Dent. Mater. **27**, 563 (2011).

[40]L. Angker and M.V. Swain, J. Mater. Res. **21**, 893 (2006).

[41]J.H. Kinney, M. Balooch, G.W. Marshall, and S.J. Marshall, Arch. Oral Biol. **44**, 813 (1999).

[42]J.L. Katz, S. Bumrerraj, J. Dreyfuss, Y. Wang, and P. Spencer, J. Biomed. Mater. Res. Appl. Biomater. **58**, 366 (2001).

[43]H. Ryou, E. Romberg, D.H. Pashley, F.R. Tay, and D. Arola, J. Mech. Behav. Biomed. Mater. **42**, 229 (2015).

[44]M. Balooch, S. Habelitz, J.H. Kinney, S.J. Marshall, and G.W. Marshall, J. Struct. Biol. **162**, 404 (2008).

[45]M. Toledano, F.S. Aguilera, E. Osorio, I. Cabello, M. Toledano-Osorio, and R. Osorio, Microsc. Microanal. **21**, 214 (2015).

[46]M. Toledano, F.S. Aguilera, E. Osorio, I. Cabello, M. Toledano-Osorio, and R. Osorio, Biointerphases **10,** 031002 (2015).